ITcon

www.itcon.org - Journal of Information Technology in Construction - ISSN 1874-4753

OCDMA-BASED SENSOR NETWORK FOR MONITORING CONSTRUCTION SITES AFFECTED BY VIBRATIONS

SUBMITTED: February 2019
REVISED: May 2019
PUBLISHED: June 2019 at https://www.itcon.org/2019/16
EDITOR: Amor R.

Farzad Pour Rahimian,
Faculty of Engineering & Environment, Northumbria University, Newcastle, UK.;
farzad.rahimian@northumbria.ac.uk

Saleh Seyedzadeh
Faculty of Engineering, University of Strathclyde, Glasgow G1 1XW, UK;
s.seyyedzadeh@gmail.com

Ivan Glesk
Faculty of Engineering, University of Strathclyde, Glasgow G1 1XW, UK;
ivan.glesk@strath.ac.uk

SUMMARY: *Due to increasing demands for the more accurate structural health monitoring of large-scale facilities, e.g. modern high-speed railways and bridges, there is a huge uptake in the development of optical sensor networks (OSN), which can help mitigate issues with conventional electric sensors, especially their sensitivity to electromagnetic interference and size. The existing fibre optic infrastructures are not widely used by OSNs, due to the lack of appropriate multiplexing techniques. Aiming at addressing the implementation issues of optical sensors in urban areas, this study proposes an efficient and cost-effective system for supporting the vibration sensing of unequally distributed points. The proposed system takes advantages of the spectral amplitude encoding optical code division multiple access (SAC-OCDMA) technique in providing differentiated services in the physical layer with varying code weights. This system utilises more wavelengths (i.e. higher power) in more distant sensing points in order to retrieve vibration signals properly. The mechanism of SAC for OSN is elaborated using simulation results, including the impact of transmission distance and the procedure for allocating codes to different zones. These results indicate the suitability of the proposed system for implementation in existing fibre optic infrastructures. Moreover, the numerical analysis shows a high capacity of the sensor network deploying SAC. The proposed system contributes to the construction research and practice by addressing the implementation issues of structural health monitoring of large-scale facilities in urban areas.*

KEYWORDS: *Structural Health Monitoring, Vibration Sensing, Optical Sensing, Optical Code Division Multiple Access, Unequally Distributed Sensor Nodes.*

REFERENCE: *Farzad Pour Rahimian, Saleh Seyedzadeh, Ivan Glesk (2019). OCDMA-based sensor network for monitoring construction sites affected by vibrations. Journal of Information Technology in Construction (ITcon), Vol. 24, pg. 299-317, http://www.itcon.org/2019/16*

1. BACKGROUND OF THE STUDY

Due to a myriad of advantages such as small and manageable size, accuracy, and immunity to electromagnetic noises, optical sensors have recently been advocated as prevailing solutions for structural health monitoring (SHM) (Majumder *et al.* 2008, Yi *et al.* 2011b). The use of optical multiplexing techniques had also improved the efficiency of optical sensing in distributed sensors networks in terms of their cost and system complexity (Li *et al.* 2004). In such systems, fibre optic sensing is either implemented as intrinsic, in which the fibre is used as the sensing element or extrinsic, where fibre is a medium to communicate the sensed signal. Seminal literature report on the success of optical sensing in the construction industry, when used for various monitoring purposes including the gas leakage (Shabaneh *et al.* 2014), temperature (Woyessa *et al.* 2016), strain (Li *et al.* 2008), reinforced concrete beams (Lu & Xie 2007) and building cladding systems (Unzu *et al.* 2013).

Accurate monitoring of vibrations is essential for assuring the structural health of large facilities in order to evaluate the structural condition and eventually mitigate risks of internal damages at very early stages, before they actually further develop and become irreversible (Li *et al.* 2004, Rinehart & Mooney 2008, Chae *et al.* 2012, Alavi *et al.* 2016). Since the use of traditional electronic sensors in measuring vibration is noticeably exposed to the electromagnetic interference, the practicality of these systems has always been only limited to a single-point simplex measurement. Researchers have taken the advantages of optical vibration sensors and their capability to eliminate the electromagnetic interference. These advantages of optical sensor networks make them more economical and allow an implementation of a broad range of essential applications for the real-time monitoring of large civil engineering structures (Barrias *et al.* 2016).

In the last decade, various fibre-optic techniques and tools have been proposed for vibration monitoring. Takahashi *et al.* (2001) employed fibre Bragg gratings (FBG) with a minimum bandwidth for a narrowband reflection of the spectrum generated by a broadband light source. The vibration was then detected based on the intensity modulation produced by the vibration of the FBG. The main disadvantage of the FBG-based sensors is their temperature sensitivity, which hinders the vibration detection. Later, a temperature compensation technique for these sensors was introduced (Gu *et al.* 2005). Zhang and Bao (2008) assessed the practicability of a fully distributed vibration sensor based on a fibre diversity detection sensor. Talebinejad *et al.* (2009) proposed an accelerometer based on FBG by exploiting the stiffness of the optical fibre. The sensor was assessed for monitoring of vibration for an actual bridge. Thakur *et al.* (2011) applied FBG and photonic crystal fibre sensors for SHM of composite and found that the crystal fibre sensor is the better alternative, as it is less sensitive to the temperature. Zhang *et al.* (2016) also monitored vibration and identified deformation distribution of a long-span rigid-frame bridge using sensors. Ge *et al.* (2013) developed a particular intensity-modulated fibre-optic accelerometer for vibration monitoring of wind turbine blades. Brillouin scattering based sensors have also been introduced for examining the distributed vibration along the optical fibre. Systems operate based on the backscattered light from the sensing fibre affected by the vibration. Since each sensor point must be accessed at a certain time slot this approach might not be the best option for a real-time vibration sensing (Hotate & Sean, 2003). Klar *et al.* (2014) evaluated a Brillouin scattering optical time domain analysis for monitoring of the tunnelling-induced ground displacements. Li *et al.* (2018) used distributed a fibre vibration sensor for monitoring pipe lines in China. They tested their approach on a system with a length of 131 km, and thousands of vibrations were detected daily.

In addition, optical sensors provide the changing characteristics of transmitted light signal over a shared media (i.e., one optical fibre), which enables multiplex measurements from multiple points to form a distributed optical sensor networks (OSN). Used multiplexing techniques include time division multiplexing (TDM) (Li *et al.* 2004), wavelength division multiplexing (WDM) (Li *et al.* 2004), frequency modulated carrier wave (Li *et al.* 2004) and optical code division multiple access (OCDMA) (Taiwo *et al.* 2014). Various multiplexing techniques to collect data from sensors have already found applications in building monitoring. WDM has commonly been used in static strain sensing and also been integrated with each other, resulting in hybrid multiplexing systems (Noura *et al.* 2013). In WDM, each sensor is assigned a given slice of the input spectrum, which is provided by a coherent optical source. WDM is mostly suitable for sensing a few points only, since by increasing the number of sensors, the system cost increases significantly due to the high cost of fabricating multi-wavelength lasers (Cheng *et al.* 2011). In time division multiplexing approach, sensors transmit signals at different time slots that demand precise network synchronisation. TDM can significantly expand the number of sensors in the time domain. Nevertheless, it endures from transmission loss and is restrained by light source power. Therefore, a few sensors (i.e. a maximum of 10 sensors) could be supported in this system (Dai *et al.* 2009). Wang *et al.* (2011) introduced a serial TDM-

OSN based on FBG and concluded that achieving high signal quality is difficult due to the presence of twelve FBGs.

Although these multiplexing methods facilitate the sensing of different structures using one shared medium, they generally fail in the utilisation of ever-growing fibre optic infrastructures in urban areas. The main reason is that OSN with current technologies are developed to monitor nodes spread over almost the same distances, so they require a separate fibre 'wiring' to avoid the retrieved vibration signals of varying powers. This results in high interference of signals. A solution must ensure received signals from different distances are with almost the same signal levels. Figure 1 illustrates an example of how sensing data from a structure can be transmitted over an urban fibre optic infrastructure.

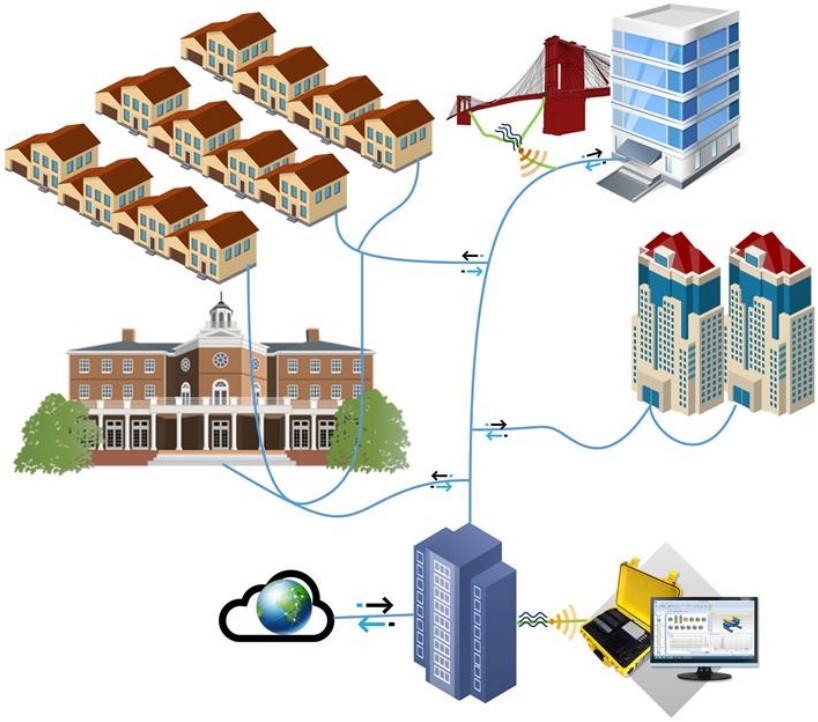

FIG. 1: Schematic demonstration of using existing urban fibre optic infrastructure for transmitting sensor data in structural monitoring.

To address these issues, several studies advocate adopting OCDMA sensor network due to its random-access capabilities (e.g. Yang & Kwong 2002, Ko *et al.* 2010, Tseng *et al.* 2013). In a sensor network based on the OCDMA system approach, each sensor will be assigned with a unique address called a signature code. This unique feature enables an individual sensor identification and provides its location in the building (Taiwo *et al.* 2016). Yen and Chih-Ming (2016) proposed an optical CDMA system to increase the capacity of OSN by integrating hybrid wavelength and time multiplexing.

The implementation of sensors in the construction industry can use either optical or electronic sensors. There have been several studies focusing on sensors placement in different structures including tower buildings (Yi *et al.* 2011a, 2012, 2014), bridges (Wan *et al.* 2013, Chen *et al.* 2014), railways (Filograno *et al.* 2010), tunnels (Li *et al.* 2008) and complex structures (Li *et al.* 2016). When it comes to sensor selection, for the vibrations monitoring, FBGs have been the choice of preference when it came to a sensor type in most OSNs, due to their low price and high performance. When it comes to a sensor placement topology, the focus has been on equally distributed sensor points. However, in SHM of structures having different distances from each other (i.e. near-far problem), it is not possible to set up the sensor network base on having equal distances from all the sensing points. The near-far problem is the inability of a receiver to hear a weak signal from a farther location in the presence of a strong signal which is transmitted from a more adjacent source. A distributed sensor network consists of varying fibre lengths connecting sensing points thus resulting in an uneven power attenuation, which makes it harder to detect the transmitting signals from faraway points with longer fibre lengths connection.

In order to address the research gap as mentioned above in supporting unequally disturbed sensors, this study proposes an optical sensing system based on a variable weight spectral amplitude coding (VW-SAC) network approach. In this system, higher weight codes (giving a better signal quality) are assigned to the nodes requiring higher quality (Prucnal 2006). The weight of the code is the number of wavelengths which are assigned to the user or sensing point. The more wavelengths will carry higher optical power. Hence, the signals from farther sensing points are carried by more power to be delivered distinguishably enough for detecting vibrations. The proposed system offers a cost-effective method for vibration monitoring of urban infrastructures such as tower buildings, bridges, tunnels. Moreover, because the SAC-OCDMA system is immune to most fibre effects (Seyedzadeh *et al.* 2016*b*), it solves the problems of WDM and TDM regarding these issues.

In this paper, a novel collimator-based VW-SAC sensor network is proposed, which is capable of supporting distributed vibration sensing while maintaining the desired signal level delivery from all monitoring nods in the network. The proposed system eliminates the demand for in-line signal amplification and thereby eases the implementation and reduces the maintenance cost of the sensing nodes located in farthest distances from the data collection point. The main advantage of this approach is that vibration monitoring of heterogeneous structures at different distances can be performed using a single sensor network by utilising inexpensive components. Furthermore, by noting the fact that optical fibres have large bandwidth, the proposed system in this study can be designed to take advantage of the possibility of using the already existing fibre infrastructure being already in place. Hence, this system presents a robust and practical vibration sensing network, ideal for monitoring of constructions in metropolitan areas where optical fibre infrastructures are readily available.

This paper first provides an overview of OCDMA and SAC systems as well as the configuration of intended distributed sensor networks (Section 2). Then the architecture of the proposed VW-SAC based sensor system is explained in detail in Section 3 providing parameters used in performance analysis. The paper also presents the results of conducted OptiSystem (Optiwave Photonics Software) simulation of the proposed sensor network based on the assumption of 3 distinct sensing points located at different distances (Section 4). The outcome of the system is also illustrated as received signals of sensors in the radio frequency domain by considering three vibration levels. The results are then expanded for a system containing nine monitoring points to demonstrate the effect of transmission distance and allocation of the right weight set to each area. Section 5 presents the results of a mathematical model, which is developed in order to drive the signal to noise ratio of received signals for showing the capacity of the proposed system in supporting simultaneous active sensors. In this mathematical model, all assumptions are set to be the worst cases in calculating an upper bound for the noise level to guarantee simulation and real case scenarios. Section 5 also presents the expansion of mathematical model and the numerical result. Finally, Section 6 presents some concluding remarks.

2. VW-SAC CODE AND ARCHITECTURE

In our proposed system, all sensing points are grouped based on the distance from the monitoring unit, where a matrix with suitable code weight is assigned to them. This means the construction sites, which are located approximately in the same distance from the control unit, are clustered in one group or zone. For example, if we have nine sensors of which four are located at the distance of 14-15 km, three at 11-12 km and two at 7-8 km away from the control unit then we will have three zones. Next, we need to assign the highest weight to the farthest zone, a lower one to the zone with the medium distance and the lowest weight to the nearest zone. In the proposed VW-SAC system, sensing points with higher weights carry vibration signals using more wavelengths or chips, hence having higher optical power. In this approach, the attenuation caused by connecting optical fibres is compensated by the increasing transmitting power by way of adding additional wavelengths instead of signal amplification. Therefore, the system can be utilised in any existing infrastructure, and without the need for any additional electric power in any given sensing location. The design of the system and choice of the codes are in a way to retrieve almost the same power from all sensing distances to overcome the near-far problem.

To determine how available chips are designated for different nodes, one needs to use one of the codes developed for SAC-OCDMA system. These codes are differentiated by their characteristics such as maximum cross-correlation (maximum number of wavelengths shared between two pairs of codes), length and supportable weight. The cross-correlation is the maximum number of overlapping wavelengths between codewords, which determines the interference level of a system. A code family with high cross-correlation provides higher information security but lower performance. The importance of using codes for sensing application rather than assigning consecutive

wavelengths to the nodes is then to provide security in the transmission layer while maintaining maximum bandwidth utilisation. The code length defines the total wavelength required for supporting the all sensing point in different zones. Generally, higher weights increase the overall code length. It is true that higher code weight intensifies the quality of one group of sensing signals, however, due to the higher length, the overall performance of the system is decreased. Therefore, to construct a system with higher capacity and still providing minimum security, it is essential to select the right code.

From several VW-code families available (Djordjevic *et al.* 2004, Kwong & Yang 2004, Liang *et al.* 2008, Anas *et al.* 2016, Seyedzadeh *et al.* 2017), this study uses VW Khazani-Syed (VW-KS) code, which was initially developed based on the single weight KS code (Ahmad Anas *et al.* 2009). KS code is based on matrix construction, where the two sub-codes A = [110] and B = [011] are used to construct the basic matrix. The structure of this code is such that a cross-correlation (the number of the overlapping chip(s) between two different users' codes), R, is either zero or one which results in the reduction of multiple access interference (MAI) effects. Figure 2 shows the basic KS code matrix with the weight of a 4. The overlapping chips between each pair of codes are depicted with blue dotted lines.

$$C_{B_4} = \begin{bmatrix} 1 & 1 & 0 & 1 & 1 & 0 & 0 & 0 & 0 \\ 0 & 1 & 1 & 0 & 0 & 0 & 1 & 1 & 0 \\ 0 & 0 & 0 & 0 & 1 & 1 & 0 & 1 & 1 \end{bmatrix}$$

$R_{1,2}=1$, $R_{1,3}=1$, $R_{2,3}=1$

FIG. 2: Construction of the basic matrix for KS code with weight of 4.

The number of rows K_B, also known as a basic number of users and number of columns N_B (basic code length), are calculated by the following equations:

$$K_B = \frac{W}{2} + 1 \tag{1}$$

and

$$N_B = 3 \sum_{i=1}^{W/2} i \tag{2}$$

For more details on constructing VW-codes for a large number of nodes refer to Appendix A.

2.1 Recovering Signals from Multiple Distances

When each sensing node's wavelengths are identified, upon a vibration exposure, these coded signals are modulated by collimators installed on the site. As all signals from all nodes travel over a shared medium, the signal in the proposed system must be optically differentiated (coded). This means that chips or wavelengths dedicated to each node should be retrieved while cancelling the effect of signals from other nodes. Then optical signals are converted into the electrical domain to obtain the vibration frequency. The more intense oscillation will result in retrieving higher frequency. This procedure will be discussed more in Section Simulation Results. Here, the approach for receiving the correct spectrum and cancelling noise is elaborated.

Among several detection techniques developed for SAC system to cancel MAI and decode the desired signals, three widely used ones are complementary subtraction (CS) detection (Zaccarin & Kavehrad 1993), AND subtraction detection (Hasoon *et al.* 2008) and direct decoding (DD) (Abdullah *et al.* 2008). Both CS and AND utilise balanced detection in which two decoders (upper and lower) are required in a single receiver to eliminate

the effect of MAI. The upper decoder detects the desired code. Using AND detection, the lower retrieves the binary logical AND of the desired and interfering code (the interfering signal from other nodes having an overlapping chip with the desired code). It recovers the complement of the upper decoder in the case of CS. DD only deploys one decoder, which reduces the number of filters and the receiver complexity.

Generally, FBGs are employed to filter the coveted wavelengths within both encoder and decoder. After forming the code words for each sensor point, the signals which have been modulated by vibration sensors travel over the fibre. In order to avoid power splitting to grab all dedicated wavelengths of the codeword, FBGs are consecutively structured in the encoder. However, such an arrangement causes unequal losses in different chips (due to the FBGs insertion loss affecting passing signals). Therefore, to prevent power reduction of various chips, in the receiver part the FBGs are arranged in the opposite order when compare to the encoder. This technique also eliminates the delay imposed by FBGs at the decoder.

The choice of deployed detection technique is dependent on the utilised code family (Seyedzadeh *et al.* 2013, 2016a). It has been shown that codes with high cross-correlation values (≥ 3) such as integer lattice optical orthogonal code (Djordjevic *et al.* 2004) are best decoded via balanced detection based methods, while DD is much appropriate for lower cross-correlation codes (e.g. VW-KS and VW-MS (Seyedzadeh *et al.* 2017)). Hence this study uses DD detection technique for retrieving the vibration modulated optical signals. The hardware experiment of a VW-OCDMA system using DD transmitted over optical fibre has been successfully demonstrated (Seyedzadeh *et al.* 2014).

3. SYSTEM DESCRIPTION

This study assumes that sensing points are distributed in different zones and the nodes residing inside the same zone have almost the same distance from the base control unit and that different zones are located unequally from the base unit. Figure 3 shows three zones with different sensing nodes and the base control unit. The main idea of this work is to assign a specific code weight for each zone where higher weights are allocated for zones with farther distance from the base. In this case, nodes are categorised into zones as equivalents to services in communication systems, according to their distances from the control unit. It should be noted that dividing nodes into the zones does not mean they are near each other but have logically distributed with similar span.

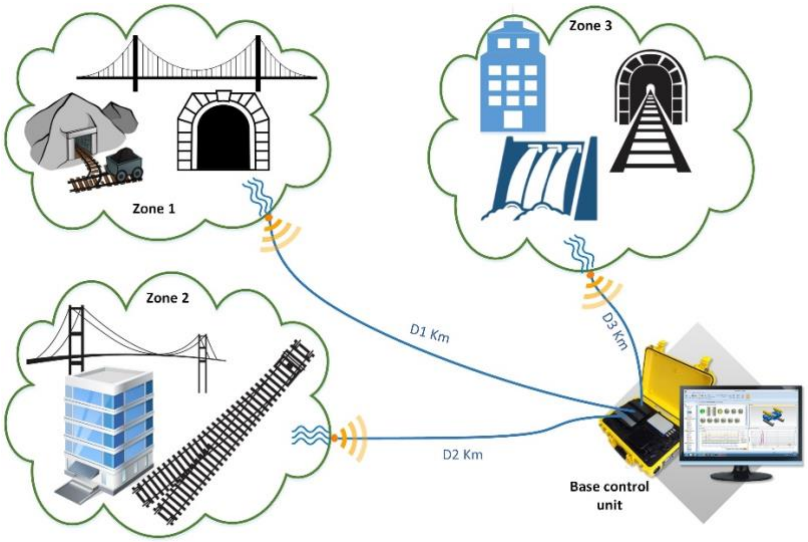

FIG. 3: Configuration of optical sensors for monitoring structures distributed over three zones with different distances from control unit.

Based on the assumed three sensing zone and nine sensing points the weight assignment technique is used to construct the desired code with weight of 6, 4 and 2.

The code structure and wavelengths assigned to individual chips are depicted in Figure 4. Nine codewords are generated using the VW-KS code with a chip spacing of 0.4 nm and a code length of 30. These codes support four sensing points in zone 3 (with the longest distance), 3 in zone 2 (with the medium distance) and 2 points in zone 1 (the nearest to the control unit).

Seq. #	Code #	W = 6																	W = 4									W = 2		
		192.2	192.25	192.3	192.35	192.4	192.45	192.5	192.55	192.6	192.65	192.7	192.75	192.8	192.85	192.9	192.95	193	193.05	193.1	193.15	193.2	193.25	193.3	193.35	193.4	193.45	193.5	193.55	193.6	193.65
1	C_1	1	1	0	1	1	0	1	1	0	0	0	0	0	0	0	0	0	0	0	0	0	0	0	0	0	0	0	0	0	0
	C_2	0	1	1	0	0	0	0	0	0	1	1	0	1	1	0	0	0	0	0	0	0	0	0	0	0	0	0	0	0	0
	C_3	0	0	0	0	1	1	0	0	0	0	1	1	0	0	0	1	1	0	0	0	0	0	0	0	0	0	0	0	0	0
	C_4	0	0	0	0	0	0	0	1	1	0	0	0	0	1	1	0	1	1	0	0	0	0	0	0	0	0	0	0	0	0
2	C_5	0	0	0	0	0	0	0	0	0	0	0	0	0	0	0	0	0	0	1	1	0	1	1	0	0	0	0	0	0	0
	C_6	0	0	0	0	0	0	0	0	0	0	0	0	0	0	0	0	0	0	0	1	1	0	0	0	1	1	0	0	0	0
	C_7	0	0	0	0	0	0	0	0	0	0	0	0	0	0	0	0	0	0	0	0	0	0	1	1	0	1	1	0	0	0
3	C_8	0	0	0	0	0	0	0	0	0	0	0	0	0	0	0	0	0	0	0	0	0	0	0	0	0	0	0	1	1	0
	C_9	0	0	0	0	0	0	0	0	0	0	0	0	0	0	0	0	0	0	0	0	0	0	0	0	0	0	0	0	1	1

FIG. 4: Code construction for vibration system and used wavelengths for each chip in OCDMA system.

Figure 5 shows the architecture of a VW-SAC OCDMA system designed for multiple sensor nodes. Amplified spontaneous emission broad-band source (ASE-BBS) is used as the optical source. The spectrum of BBS is sent through an optical circulator and a 1×3 optical coupler (for supporting three zones). Each coupler port is then connected to a 1×N coupler (N is the number of sensing point in each zone) after transmission over a single mode fibre (SMF) with different lengths of 8, 12 and 15 km, respectively. Then output ports of secondary couplers are connected to sensing points to collect vibration signals. The encoder of VW-SAC comprises a collimator, vibration box and a series of FBGs. Due to the property of VW-KS code in being double weighted, the two wavelengths can be reflected using one FBG with bandwidth twice the chip spacing. The generated vibration causes a modulation that can be detected by decoders. In conducted simulation set-up, the study uses a Mach Zehnder modulator to mimic the behaviour of the collimator in sensing the vibration. Three different frequencies of 70, 140 and 210 MHz are used to represent low, medium and high vibration, respectively. It should be noted that these values are examples from previous experimental researches Taiwo et al. (2016) and are used to demonstrate the operation of the proposed system. In a real-world implementation, first, the intensity of vibration is not discrete and second the range is determined by the type of the structure and variation of the quiver.

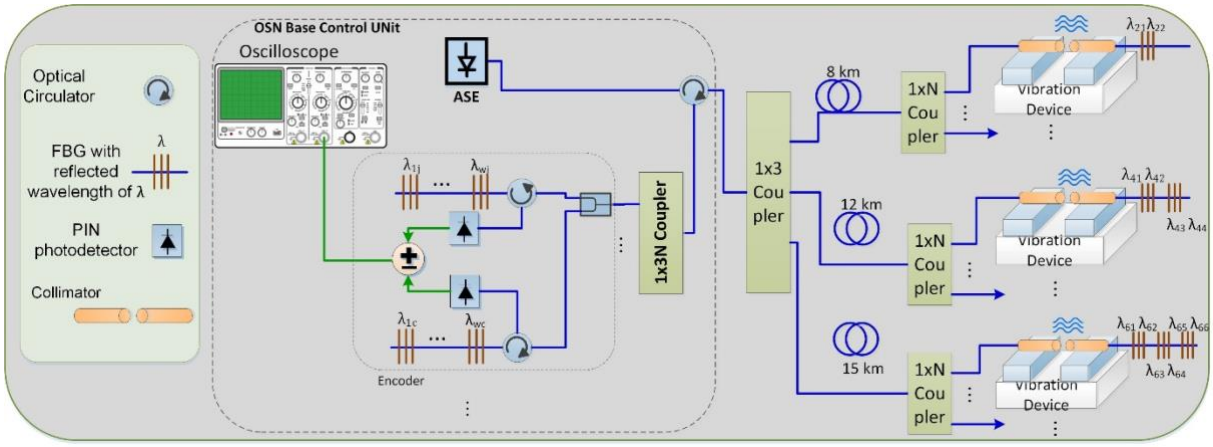

FIG. 5: VW-SAC OCDMA system structure of fibre vibration sensor for monitoring three nodes in different areas.

As indicated in Figure 5, vibration modulated signals traveling back are first recombine by the couplers and then guided to the detection section by an optical circulator. Here, the combined signals are split by a 1×N coupler and fed into decoder. Here, FBGs are used to filter out the desired wavelengths for the receiver. As mentioned, DD is used for recovery of sensor signals in which only the non-overlapping wavelengths (chips without cross-correlation with other codes) are detected at the receiver for the desired 'users'. As the node with weight 2 uses only one filter in both encoder and decoder, the order is not important.

The decoded optical signals are finally converted into the electrical domain employing PIN photodetectors and sent to three channel oscilloscopes with fast Fourier transform capabilities.

The proposed system is simulated using OptiSystem version 12 software and default values are used for optical and electrical components.

4. SIMULATION RESULTS

Three different vibration scenarios are considered to demonstrate the performance of the system as shown in Table 1. To illustrate the vibration sensing in the system from each zone one sensing point is selected. Nodes N_1, N_2 and N_3 are respectively located 8, 12 and 15 km far from the base control unit. The frequencies of other nodes are randomly assigned from 0 to 210 MHz.

Table 1: Configuration of vibration frequencies for three nodes indicating various vibration scenarios for these points

Node	EXP 1 (MHz)	EXP 2 (MHz)	EXP 2 (MHz)
N_1 (W =2)	70	0	210
N_2 (W =4)	140	70	70
N_3 (W =5)	210	210	70

Figure 6(a) to 6(c) illustrate the power represented in a radio frequency (RF) domain received from three nodes in experiments 1 to 3, respectively. As it can be observed low, medium and high vibration signal is constantly retrieved at frequencies of 66.3, 139.8 and 207.1 MHz at the encoder. Moreover, the signals of all nodes in different configurations are revived at almost the same peak power (±1 dB). The configuration of utilised weights are based on the selected distances and different combination can be applied for desired results.

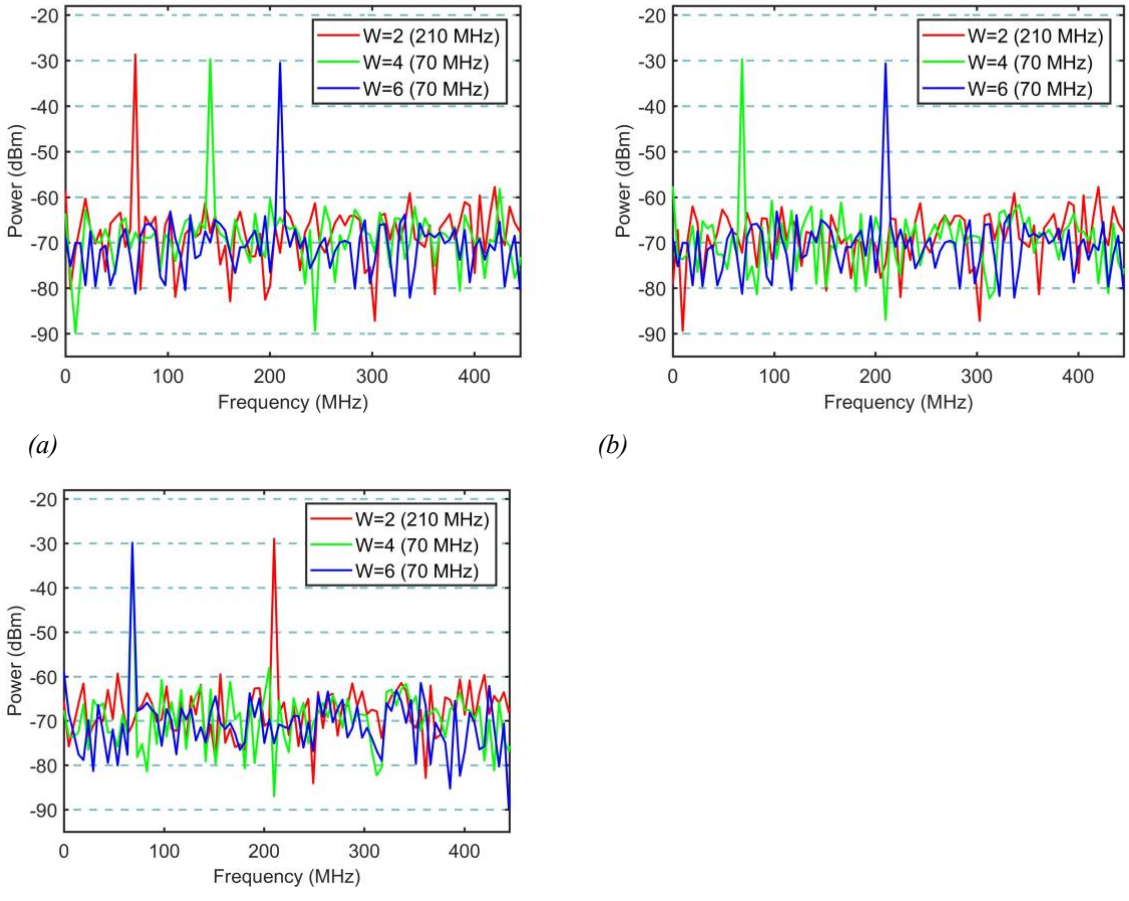

(a) *(b)*

(c)

FIG. 6: The RF signal power received for three nodes for experiments (a)1 - (c) 3 indicated in Table 1.

Hence, the weight of each zone is selected in a way that sufficient optical power for delivery of a noiseless signal could be received by the base station when all signals are collected, and the vibration is monitored.

To make it clear, another experiment was conducted to check the scenario in which different weights are applied to the same distance. Here, the fibre length for all nodes is set to 20 km and the vibration frequencies are adopted from experiment 1 in Table 1. Figure 7 depicts the signal power for different frequencies. The signal for node N_3 which is received with a power of -33.4 dBm, so the vibration is distinctly detectable. The signals from node N_1 and node N_2 are obtained with peak power of -47.6 and -41.8 dBm, respectively. The power retrievals are lower than for node N_3 as they are assigned lower weights. This shows that it would be impossible to recognise vibrations happening in node N_1 with its present configuration.

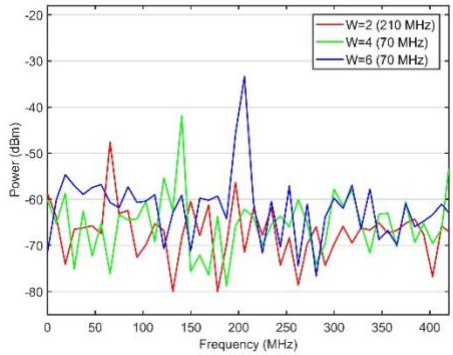

FIG. 7: The RF signal power received for distance of 20 km for all nodes.

4.1 Effect of Transmission Distance

In order to evaluate the performance of the proposed system under the influence of the transmission medium, a set-up with nine nodes (two points in the nearest zone with the allocated weight of 2, three points in zone 2 with the weight of 4 and four-point at the farthest zone with weight 6) is investigated. The codes are generated using the fixed mapping technique (cf. Appendix A). The plot of the signal to noise ratio (SNR) against the average transmission distance is presented in Figure 8. The different length of optical fibre for each zone is represented by the x-axis.

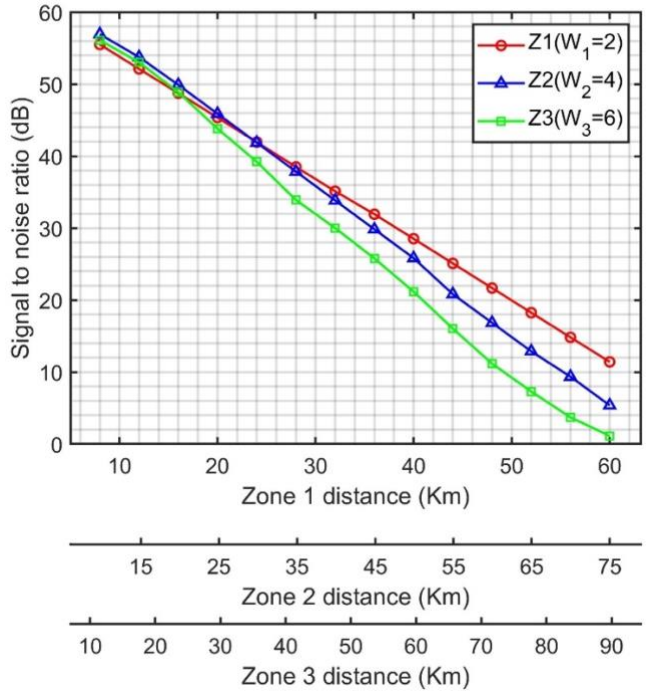

FIG. 8: SNR of received signals from three zones vs transmission distance.

It can be seen that below the transmission distance of 56 km, SNRs of all nodes satisfy the minimum value of 15 dB. The reason why SNRs for nodes with higher weights decrease with a faster rate depends on fibre properties (Seyedzadeh *et al.* 2016b). To obtain robust results, the worst-case scenarios are selected for investigations. Since in the practice, the vibration frequencies are far lower than the test cases in this study the chirping effect due to fibre dispersion will not be detrimental. Therefore, for the metropolitan area size networks, not in-line boosting, nor dispersion compensation is needed.

To elaborate on the determination of the right weight for different distances, this study assumes that the zone 3 (zone 2) is located at a distance which is 2 and 2.5 times larger than the zone 1 distance from the control unit, respectively. The aim is to assign weights for these three zones located at 36, 72 and 90 km from the data collection point. Figure 9 demonstrates two sets of weights allocated for 9 sensor points distributed in different zones. The first set (i.e. 6, 4 and 2) cannot deliver good enough signal quality for nodes located in zone 2 and 3. Utilising the second set by including weights 10, 8 and 2, signals from all nodes are received with a sufficient power level and acceptable SNRs. That means the second set of weights allows for monitoring of vibrations of structures located at the targeted distances. Hence in summary, the selection of weights for each zone depends on distances of all zones from the signal collection point, and the number of sensing points located in each area.

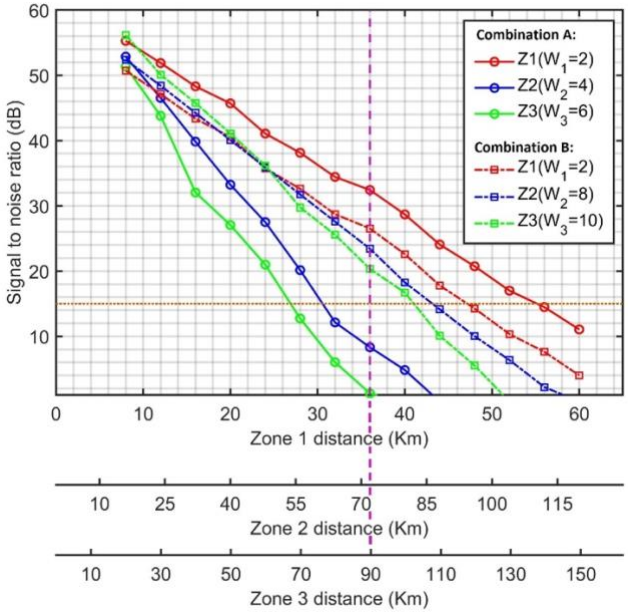

FIG. 9: SNR for different combination of code weights against transmission distance.

5. VW-OCDMA SENSOR SYSTEM CAPACITY

In order to determine the approximate capacity of VW-OCDMA sensor system, a mathematical model based on the upper bound calculation (Smith *et al.* 1998) is developed. In this model, shot and thermal noises are taken into account to derive the SNR of the received signals. It should be noted that as DD detection is used, the phase-induced intensity noise is avoided.

The noise variance of a photocurrent emitted from the optical source as a result of the detection of an ideally unpolarised thermal light can be calculated as (Wei *et al.* 2001):

$$\langle I^2 \rangle = \langle I_{shot}^2 \rangle + \langle I_{thermal}^2 \rangle \quad (3)$$

Where I_{shot} and $I_{thermal}$ represent the shot and thermal noise, respectively. The coherence time of the thermal source, τc is given by (Smith *et al.* 1998)

$$\tau_c = \frac{\int_0^\infty G^2(v)dv}{\left[\int_0^\infty G^2(v)dv\right]^2} \tag{4}$$

Where $G(v)$ is the source power spectral density (PSD).

This mathematical model considers following assumptions:

a) Each power spectral component has an identical spectral width.
b) Each node receives equal amount of the total power.
c) Each vibration is considered as a modulated signal at a frequency of 210 MHz.
d) The number of nodes in every zone is almost the same

The PSD of the received signals can be expressed as (Yang *et al.* 2004):

$$r(v) = \frac{P_{sr}}{\Delta v}\sum_{k=1}^{K} d_k \sum_{i=1}^{N} c_k(i)\Pi(i) \tag{5}$$

Here P_{sr} is the effective power of the source at the receiver, Δv is the bandwidth of the optical source, K and N are the number of sensor nodes and total code length, respectively, d_k is the modulated information of k-th vibrated node which is either "1" or "0", $(d_k \epsilon 0, 1)$, $c_k(i)$ is the i-th element of the k-th KS code sequence and $\Pi(i)$ is a function written as:

$$\begin{aligned}\Pi(i) = u\left[v - v_0 - \frac{\Delta v}{2N}(-N+2i-2)\right] - \\ u\left[v - v_0 - \frac{\Delta v}{2N}(-N+2i)\right] \\ = u\left[\frac{\Delta v}{2N}\right]\end{aligned} \tag{6}$$

and $u[v]$ is the unit step function expressed as:

$$u[v] = \begin{cases} 1, & v \geq 0 \\ 0, & v < 0 \end{cases} \tag{7}$$

The code properties using DD is expressed as

$$\sum_{i=1}^{N} c_k(i)c_l(i) = \begin{cases} W_k/2, & k = l \\ 0, & k \neq l \end{cases} \tag{8}$$

The photocurrent of the desired node's signal is therefore

$$I_R = \frac{\Re P_{sr} W_k}{2N_v} \tag{9}$$

Where $\Re$ represents the receiver responsivity, and P_{sr} is the received power. It is assumed that the configuration of the VW-OCDMA sensor system guarantees that signals arriving from nodes at different distances are received with almost the same power, therefore $P_{sr} \times W_k$ remains constant for all nodes and can be replaced by P_c. Indeed, this is the main idea of varying weights for the unequally distributed sensors. For longer distances P_{sr} is decreased; however, different higher weights, W_k, ensure that the same received power will be attained from these nodes. The noise level in all signals carried by different wavelengths is not the same even with equal optical power. However, as this model gives an upper bound approximation of SNR, this issue can be ignored.

The variance of shot noise in the photocurrent can be calculated as

$$\left\langle I_{shot}^2 \right\rangle = \frac{eB\Re P_c}{N_v} \tag{10}$$

The thermal noise is given as

$$\left\langle I_{thermal}^2 \right\rangle = \frac{4K_b T_n B}{R_L} \tag{11}$$

where B is the electrical bandwidth, K_b is Boltzmann's constant, T_n is received noise temperature and R_L represents the receiver load resistance.

Hence, the SNR for VW-SAC-OCDMA can be written as

$$\begin{aligned} SNR &= \frac{I_R}{\langle I_{shot}^2 \rangle + \langle I_{thermal}^2 \rangle} \\ &= \frac{\frac{\Re^2 P_c^2}{2N_v^2}}{\frac{eB\Re P_c}{N_v} + \frac{4K_b T_n B}{R_L}} \end{aligned} \tag{12}$$

The parameters for the mathematical analysis are listed in Table 2.

Table 2: The mathematical parameters adopted from (Kakaee et al. 2014, Smith et al. 1998, Shalaby 2012) used in the evaluation of system capacity.

Symbol	Parameter	Value
Symbol	Parameter	Value
η	Photodetector quantum efficiency	0.6
Δv	The linewidth of the broadband source	3.75 THz
λ_0	Operating wavelength	1550 nm
P_c	Received optical power	-10 dBm
T_n	Receiver noise temperature	300 K
R_l	Receiver load resistor	1030 Ω
e	Electron charge	1.6×10^{-19} C
h	Planck's constant	6.66×10^{-34} Js
K_b	Boltzmann's constant	1.38×10^{-23} J/K

Figure 10 shows the plot of SNR versus the number of simultaneous sensor nodes with different configurations. The three zones configuration is simulated using (6, 4, 2), (8, 6, 4) and (10, 6, 4) code combinations. The system capacity is also illustrated for four zones with assigned code weights of 8, 6, 4 and 2. It can be seen that how increasing the code weight expand the system capacity.

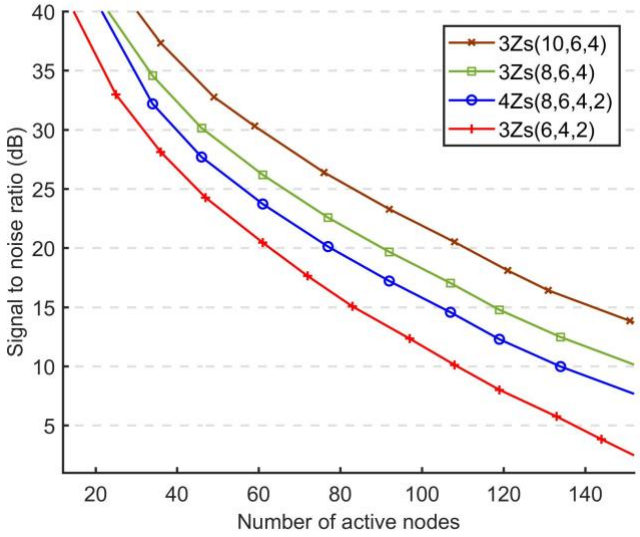

FIG. 10: SNR of received signal against number of active nodes in the system.

It could be concluded that, different configurations can be designed for each specific optical sensor network with various number of zones and sensing points. In this analysis, it was assumed that each node group (zone) with a different weight has the same share of the total number of nodes. However, it should be noted that if the number of nodes with lower weights are dominant, the system capacity will increase due to the reduction of the total code length, N_v and vice versa. The diagram shown in Figure 11 illustrates a rule of thumb approach to select the code weights for the required number of zones and the sensing points.

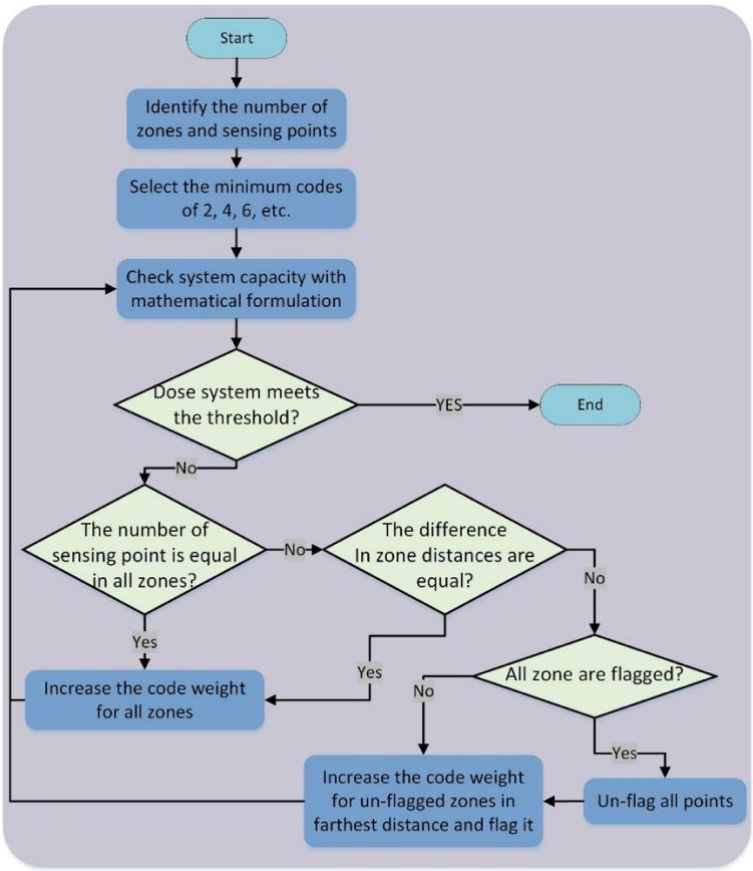

FIG. 11: Flowchart for selecting code weight Deleted because if kept there will need more explanation.

To support a large number of nodes distributed across several zones, the use of more flexible OCDMA codes such as VW-MS (Seyedzadeh *et al.* 2017), will result in a better SNR and more flexible code construction for the desired configuration.

6. CONCLUSION

The research presented in this study addresses the functionality gap between the emerging optical sensor networks and urban SHM, in order to leverage more efficient remote vibration sensing of constructed sites. As mentioned in the reviewed literature, despite the broad adoption of the optical sensing in SHM, there are several challenges in monitoring various structures located in urban areas. This includes high cost of the implementation of WDM systems, the demand for synchronisation in TDM networks and the inability of sensing to support of various zones which are distributed in the urban area without the need for independent connectivity. This study is our response to address the need for the cost-effective monitoring by utilizing the existing infrastructure and fibre links which are connecting these dispersed construction areas while minimizing possible detrimental effects arising from nonlinearities due to the signal amplification, dispersion, and time jitter - effects which otherwise would need to be carefully dealt with in case of employing competing approaches, including WDM or TDM systems. The proposed VW-SACOCDMA does not require any traffic management or system synchronisation and was shown in Section Effect of Transmission Distance, is also resilient to performance degradations caused by fibre nonlinearities.

The proposed optical multiplexing system for monitoring vibration in unequally distributed nodes, is based on a VW-SAC OCDMA. The proposed system with nine nodes with different distances from the control unit was then investigated, using optical simulation software. Low, medium and high vibrations were considered as a sinusoidal modulation with different frequency. The corresponding received signals were presented in the radio frequency domain for three nodes in different zones. The results indicate that the applied vibration frequencies were explicitly obtained for all weights in various scenarios. Furthermore, the conducted simulation showed how by increasing the fibre length (i.e. the distance of nodes from the base) nodes with the lower weight experience more signal power degradation would make the vibration detection more difficult. The combine effect of transmission fibre and selection of an appropriate code for different zones are numerically analysed by considering nine sensing points distributed in three locations. Moreover, through mathematical approximation, the capacity of VW-OCDMA for vibration sensing was demonstrated as SNR against the number of nodes; obtained results indicate that the proposed system has the potential to support a high number of nodes distributed with uneven distances. The performance of the system may be further improved using more flexible OCDMA code families. The simulation and mathematical results point out the suitability of the VW-OCDMA system vibration sensing with a simple implementation and high accuracy. If the security of monitoring data is not an issue, the use of zero cross-correlation codes is recommended as they provide a better code-word cardinality while using the same bandwidth.

ACKNOWLEDGEMENT

This project has received funding from the European Union's Horizon 2020 research and innovation program under the Marie Sklodowska-Curie grant agreement No 734331.

REFERENCES

Abdullah, M. K., Hasoon, F. N., Aljunid, S. A. & Shaari, S. (2008), 'Performance of OCDMA systems with new spectral direct detection (SDD) technique using enhanced double weight (EDW) code', Optics Communications 281(18), 4658– 4662.

Ahmad Anas, S. B., Abdullah, M. K., Mokhtar, M., Aljunid, S. A. & Walker, S. D. (2009), 'Optical domain service differentiation using spectral-amplitude-coding', Optical Fiber Technology 15(1), 26–32.

Alavi, A. H., Hasni, H., Lajnef, N., Chatti, K. & Faridazar, F. (2016), 'An intelligent structural damage detection approach based on self-powered wireless sensor data', Automation in Construction 62, 24–44.

Anas, S. B. A., Seyedzadeh, S., Mokhtar, M. & Sahbudin, R. K. Z. (2016), 'Variable weight Khazani-Syed code using hybrid fixed-dynamic technique for optical code division multiple access system', Optical Engineering 55(10), 106101.

Barrias, A., Casas, J., & Villalba, S. (2016). A review of distributed optical fiber sensors for civil engineering applications. Sensors, 16(5), 748.

Chae, M. J., Yoo, H. S., Kim, J. Y. & Cho, M. Y. (2012), 'Development of a wireless sensor network system for suspension bridge health monitoring', Automation in Construction 21(1), 237–252.

Chen, B., Wang, X., Sun, D. & Xie, X. (2014), 'Integrated system of structural health monitoring and intelligent management for a cable-stayed bridge.', The Scientific World JournalWorldJournal 2014, 689471.

Cheng, H. C., Wu, C. H., Yang, C. C. & Chang, Y. T. (2011), 'Wavelength division multiplexing/spectral amplitude coding applications in fiber vibration sensor systems', IEEE Sensors Journal 11(10), 2518–2526.

Dai, Y., Liu, Y., Leng, J., Deng, G., & Asundi, A. (2009). A novel time-division multiplexing fiber Bragg grating sensor interrogator for structural health monitoring. Optics and Lasers in Engineering, 47(10), 1028-1033.

Djordjevic, I. B., Vasic, B. & Rorison, J. (2004), 'Multi-weight unipolar codes for multimedia spectral-amplitude-coding optical CDMA systems', IEEE Communications Letters 8(4), 259–261.

Filograno, M. L., Corredera Guillen, P., Rodriguez-Barrios, A., Martin-Lopez, S., Rodriguez-Plaza, M., Andres-Alguacil, A. & Gonzalez-Herraez, M. (2010), RealTime Monitoring of Railway Traffic Using Fiber Bragg Grating Sensors, in 'Joint Rail Conference', Vol. 2, American Society of Mechanical Engineers, pp. 27–29.

Ge, Y., Kuang, K. S., & Quek, S. T. (2013). Development of a low-cost bi-axial intensity-based optical fibre accelerometer for wind turbine blades. Sensors and Actuators A: Physical, 197, 126-135.

Guo, T., Zhao, Q., Dou, Q., Zhang, H., Xue, L., Huang, G., & Dong, X. (2005). Temperature-insensitive fiber Bragg grating liquid-level sensor based on bending cantilever beam. IEEE photonics technology letters, 17(11), 2400-2402.

Hasoon, F. N., Aljunid, S. A., Samad, M. D. A., Abdullah, M. K. & Shaari, S. (2008), 'Spectral amplitude coding OCDMA using AND subtraction technique', Applied Optics 47(9), 1263.

Hotate, K., & Ong, S. S. (2003). Distributed dynamic strain measurement using a correlation-based Brillouin sensing system. IEEE Photonics Technology Letters, 15(2), 272-274.

Kakaee, M. H., Seyedzadeh, S., Adnan Fadhil, H., Barirah Ahmad Anas, S. & Mokhtar, M. (2014), 'Development of Multi-Service (MS) for SAC-OCDMA systems', Optics & Laser Technology 60, 49–55.

Klar, A., Dromy, I., & Linker, R. (2014). Monitoring tunneling induced ground displacements using distributed fiber-optic sensing. Tunnelling and Underground Space Technology, 40, 141-150.

Ko, J., Kim, Y. & Park, C.-S. (2010), 'Fiber Bragg grating sensor network based on code division multiple access using a reflective semiconductor optical amplifier', Microwave and Optical Technology Letters 52(2), 378–381.

Kwong, W. & Yang, G.-C. (2004), 'Multiple-Length Multiple-Wavelength Optical Orthogonal Codes for Optical CDMA Systems Supporting Multirate Multimedia Services', IEEE Journal on Selected Areas in Communications 22(9), 1640–1647.

Li, C., Zhao, Y. G., Liu, H., Wan, Z., Zhang, C. & Rong, N. (2008), 'Monitoring second lining of tunnel with mounted fiber Bragg grating strain sensors', Automation in Construction 17(5), 641–644.

Li, G., Zhu, J., Sun, R., Lin, X., Yang, W., Zeng, K., Wang, F., Wang C., & Zhou, B. (2018). Pipe Line Safety Monitoring using Distributed Optical Fiber Vibration Sensor in the China West-East Gas Pipeline Project. In 2018 Asia Communications and Photonics Conference (ACP) (pp. 1-3). IEEE.

Li, H. N., Li, D. S. & Song, G. B. (2004), 'Recent applications of fiber optic sensors to health monitoring in civil engineering', Engineering Structures 26(11), 1647– 1657.

Li, H.-N., Ren, L., Jia, Z.-G., Yi, T.-H. & Li, D.-S. (2016), 'State-of-the-art in structural health monitoring of large and complex civil infrastructures', Journal of Civil Structural Health Monitoring 6(1), 3–16.

Liang, W., Yin, H., Qin, L., Wang, Z. & Xu, A. (2008), 'A new family of 2D variableweight optical orthogonal codes for OCDMA systems supporting multiple QoS and analysis of its performance', Photonic Network Communications 16(1), 53– 60.

Lu, S.-w. & Xie, H.-q. (2007), 'Strengthen and real-time monitoring of RC beam using intelligent CFRP with embedded FBG sensors', Construction and Building Materials 21(9), 1839–1845. URL: http://linkinghub.elsevier.com/retrieve/pii/S095006180600239X

Majumder, M., Gangopadhyay, T. K., Chakraborty, A. K., Dasgupta, K. & Bhattacharya, D. K. (2008), 'Fibre Bragg gratings in structural health monitoringPresent status and applications'.

Noura, A., Seyedzadeh, S. & Anas, S. B. (2013), Simultaneous vibration and humidity measurement using a hybrid WDM/OCDMA sensor network, in '4th International Conference on Photonics, ICP 2013 - Conference Proceeding', IEEE, pp. 163–165.

Optiwave Photonics Software (n.d.), 'OptiSystem Overview'. URL: https://optiwave.com/optisystem-overview/

Prucnal, P. R. (2006), OPTICAL CODE DIVISION MULTIPLE ACCESS Fundamentals and Applications, CRC Taylor & Francis.

Rinehart, R. V. & Mooney, M. A. (2008), 'Instrumentation of a roller compactor to monitor vibration behavior during earthwork compaction', Automation in Construction 17(2), 144–150. URL: http://linkinghub.elsevier.com/retrieve/pii/S0926580506001294

Seyedzadeh, S., Mahdiraji, G. A., Sahbudin, R. K. Z., Abas, A. F. & Anas, S. B. A. (2014), 'Experimental demonstration of variable weight SAC-OCDMA system for QoS differentiation', Optical Fiber Technology 20(5), 495–500.

Seyedzadeh, S., Moghaddasi, M. & Anas, S. (2016a), 'Variable-weight optical code division multiple access system using different detection schemes', Journal of Telecommunications and Information Technology 2016(3).

Seyedzadeh, S., Moghaddasi, M. & Anas, S. B. A. (2016b), 'Effects of fibre impairments in variable weight optical code division multiple access system', IET Optoelectronics 10(6), 221–226.

Seyedzadeh, S., Rahimian, F. P., Glesk, I. & Kakaee, M. H. (2017), 'Variable weight spectral amplitude coding for multiservice OCDMA networks', Optical Fiber Technology 37, 53–60.

Seyedzadeh, S., Sahbudin, R. K., Abas, A. F. & Anas, S. B. (2013), Weight optimization of variable weight OCDMA for triple-play services, in '4th International Conference on Photonics, ICP 2013 - Conference Proceeding', IEEE, Melaka, pp. 99–101.

Shabaneh, A., Girei, S., Arasu, P., Rahman, W., Bakar, A., Sadek, A., Lim, H., Huang, N. & Yaacob, M. (2014), 'Reflectance response of tapered optical fiber coated with graphene oxide nanostructured thin film for aqueous ethanol sensing', Optics Communications 331, 320–324. URL: http://linkinghub.elsevier.com/retrieve/pii/S0030401814005823

Shalaby, H. H. M. (2012), 'Closed-Form Expression for the Bit-Error Rate of Spectral-Amplitude-Coding Optical CDMA Systems', IEEE Photonics Technology Letters 24(15), 1285–1287.

Smith, E. D. J., Blaikie, R. J. & Taylor, D. P. (1998), 'Performance Enhancement of Spectral- Amplitude-Coding Optical CDMA Using Pulse-Position Modulation', IEEE Transactions on Communications 46(9), 1176–1185.

Taiwo, A., Moghaddasi, M., Kuje, D., Idriss, Y. & Mokhtar, M. (2016), 'Practical investigation of suitable decoding techniques for spectral amplitude coding optical code division multiple access-based vibration sensing', IET Optoelectronics 10(6), 227–232.

Taiwo, A., Seyedzadeh, S., Taiwo, S., Sahbudin, R. K. Z., Yaacob, M. H. & Mokhtar, M. (2014), 'Performance and comparison of fiber vibration sensing using SACOCDMA with direct decoding techniques', Optik - International Journal for Light and Electron Optics 125(17), 4803–4806.

Takahashi, N., Yoshimura, K., & Takahashi, S. (2001). Fiber Bragg grating vibration sensor using incoherent light. Japanese Journal of Applied Physics, 40(5S), 3632.

Talebinejad, I., Fischer, C., & Ansari, F. (2009). Serially multiplexed FBG accelerometer for structural health monitoring of bridges. Smart Structures and Systems, 5(4), 345-355. Tseng, S.-P., Yen, C.-T., Syu, R.-S. & Cheng, H.-C. (2013), 'Employing optical code division multiple access technology in the all fiber loop vibration sensor system', Optical Fiber Technology 19(6), 627–637. URL: http://www.sciencedirect.com/science/article/pii/S1068520013001272

Thakur, H. V., Nalawade, S. M., Saxena, Y., & Grattan, K. T. V. (2011). All-fiber embedded PM-PCF vibration sensor for Structural Health Monitoring of composite. Sensors and Actuators A: Physical, 167(2), 204-212.

Unzu, R., Nazabal, J. A., Vargas, G., Hern´andez, R. J., Fern´andez-Valdivielso, C., Urriza, N., Galarza, M. & Lopez-Amo, M. (2013), 'Fiber optic and KNX sensors network for remote monitoring a new building cladding system', Automation in Construction 30, 9–14.

Wan, C., Hong, W., Liu, J., Wu, Z., Xu, Z. & Li, S. (2013), 'Bridge assessment and health monitoring with distributed long-gauge FBG sensors', International Journal of Distributed Sensor Networks 2013(12), 494260.

Wang, Y., Gong, J., Wang, D. Y., Dong, B., Bi, W., & Wang, A. (2011). A quasi-distributed sensing network with time-division-multiplexed fiber Bragg gratings. IEEE Photonics Technology Letters, 23(2), 70-72.

Wei, Z., Shalaby, H. M. H. & Ghafouri-Shiraz, H. (2001), 'Modified quadratic congruence codes for fiber Bragg-grating-based spectral-amplitude-coding optical CDMA systems', Journal of Lightwave Technology 19(9), 1274–1281.

Woyessa, G., Nielsen, K., Stefani, A., Markos, C. & Bang, O. (2016), 'Temperature insensitive hysteresis free highly sensitive polymer optical fiber Bragg grating humidity sensor', Optics Express 24(2), 1206. URL: https://www.osapublishing.org/abstract.cfm?URI=oe-24-2-1206

Yang, C.-C., Huang, J.-F., Tseng, S.-P., Chao-Chin, Y., Jen-Fa, H. & Shin-Pin, T. (2004), 'Optical CDMA network codecs structured with M-sequence codes over waveguide-grating routers', Photonics Technology Letters, IEEE 16(2), 641–643.

Yang, G. C. & Kwong, W. C. (2002), Prime codes with applications to CDMA optical and wireless networks, Artech House.

Yen, Chih-Ta, and Chih-Ming Chen. "A study of three-dimensional optical code-division multiple-access for optical fiber sensor networks." Computers & Electrical Engineering 49 (2016): 136-145.

Yi, T.-H., Li, H.-N. & Gu, M. (2011a), 'A new method for optimal selection of sensor location on a high-rise building using simplified finite element model', Structural Engineering and Mechanics 37(6), 671–684.

Yi, T.-H., Li, H.-N. & Gu, M. (2011b), 'Optimal sensor placement for structural health monitoring based on multiple optimization strategies', The Structural Design of Tall and Special Buildings 20(7), 881–900.

Yi, T. H., Li, H. N. & Zhang, X. D. (2012), 'Sensor placement on Canton Tower for health monitoring using asynchronous-climb monkey algorithm', Smart Materials and Structures 21(12), 125023.

Yi, T.-H., Li, H.-N. & Zhang, X.-D. (2014), 'Health monitoring sensor placement optimization for Canton Tower using immune monkey algorithm', Structural Control and Health Monitoring 22(1), 123–138.

Zaccarin, D. & Kavehrad, M. (1993), 'An Optical CDMA System Based on Spectral Encoding of LED', IEEE Photonics Technology Letters 5(4), 479–482.

Zhang, J., Tian, Y., Yang, C., Wu, B., Wu, Z., Wu, G., Zhang, X. and Zhou, L (2016). Vibration and deformation monitoring of a long-span rigid-frame bridge with distributed long-gauge sensors. Journal of Aerospace Engineering, 30(2), B4016014.

Zhang, Z., & Bao, X. (2008). Continuous and damped vibration detection based on fiber diversity detection sensor by Rayleigh backscattering. Journal of Lightwave Technology, 26(7), 832-838.

Zhou, Z. and Ou, J., 2005, June. Techniques of temperature compensation for FBG strain sensors used in long-term structural monitoring. In Fundamental Problems of Optoelectronics and Microelectronics II (Vol. 5851, pp. 167-173). International Society for Optics and Photonics.

APPENDIX A. EXPANDING OCDMA CODE FOR EXTENTED NUMBER OF SENSORS

The process of VW-KS code construction is a combination of two algorithms, which are fixed mapping technique and dynamic weight assignment. The first technique is a simple mapping of codes with same and different weights that had been initially constructed using single weight KS technique. The second technique, dynamic weight assignment uses the value of [1 2 1] combination to arrange sub-codes A and B, accordingly (Anas *et al.* 2016). The main aim of developing dynamic weight assignment was to support few number of differentiated services without wasting extra bandwidth.

A.1. Mapping technique

First, the number of sensor points is increased by mapping the basic matrix, C_B, for the required weight. Based on the assumption that the total number of requisite sensors in one region (which determines the allocated weight) is N, the basic matrix repeated by $M = \lfloor N/N_B c \rfloor$times, where N_B is the number of nodes in C_B as the following matrix:

$$C(M) = \begin{bmatrix} C_B(1) & 0 & 0 & 0 & 0 \\ 0 & C_B(2) & 0 & 0 & 0 \\ 0 & 0 & C_B(3) & 0 & 0 \\ 0 & 0 & 0 & \ddots & 0 \\ 0 & 0 & 0 & 0 & C_B(M) \end{bmatrix}$$

here $C_B(m)$ is the mth mapping sequence where m = 1,2,...,M. Each '0' in the mapping matrix is a sequence of zeros with the same size of C_B. The maximum crosscorrelation λ_c between codes within the same matrix is one and from different mappings is zero. Hence; using the mapping technique maximum cross-correlation of 1 obtained for all users.

Therefore, sensor points are grouped based on the distance from the monitoring unit where a matrix with suitable code weight is assigned for them. This means the construction sites which are located approximately in the same distance from the control unit are clustered in one zone. For example, if we have nine sensors of which four located in almost 18-20 km, 3 in 12-5 km and 2 from 8-10 km from the control unit, then we will have three zones. Next, we need to assign the highest weight to the farthest zone, a lower one to the zone with the medium distance and the lowest weight to the nearest zone.

A matrix with the desired code weight is assigned to each zone. As it is discussed if the number of points is higher than one basic matrix, more number of mapped matrices are assigned to the group to support all users. Then, matrices with different code weights are joined together using the mapping method to construct the overall matrix. Figure 12, illustrates the structure of VW-code construction to support Q number of multiple distances (weights) using KS code. $C_{BW_q}(m)$ shows the mth mapping basic matrix for qth region which is appointed with the weight of W_q.

$$\begin{bmatrix} \begin{bmatrix} C_{Bw_1}(1) & 0 & 0 \\ 0 & \ddots & 0 \\ 0 & 0 & C_{Bw_1}(M_1) \end{bmatrix} & 0 & 0 \\ 0 & \begin{bmatrix} C_{Bw_2}(1) & 0 & 0 \\ 0 & \ddots & 0 \\ 0 & 0 & C_{Bw_2}(M_2) \end{bmatrix} & 0 \\ 0 & 0 & \ddots \\ 0 & 0 & 0 \end{bmatrix} \quad \begin{matrix} 0 \\ 0 \\ 0 \\ \begin{bmatrix} C_{Bw_Q}(1) & 0 & 0 \\ 0 & \ddots & 0 \\ 0 & 0 & C_{Bw_Q}(M_{jQ}) \end{bmatrix} \end{matrix}$$

FIG. 12: General structure of VW-Code construction using KS code.

The total code length of VW-MS code, Lt with mapping technique is expressed as:

$$L_t = \sum_{q=1}^{Q} \left(\left(M_q \times 3 \sum_{i=1}^{W_q/2} i \right) \right) \tag{A.1}$$

A.2. Dynamic weight assignment and hybrid method

Dynamic weight assignment reduces the code length by considering two important parameters to determine the position of sub-codes insertion. They are the value of 3-column combination (3CC) and cross-correlation between two different users, x and y, i.e. $R_{x,y}$. Figure 13 shows an example of KS codes with illustration of 3CC and $R_{x,y}$ values. The procedure of dynamic weight assignment is elaborated by Anas *et al.* (2016).

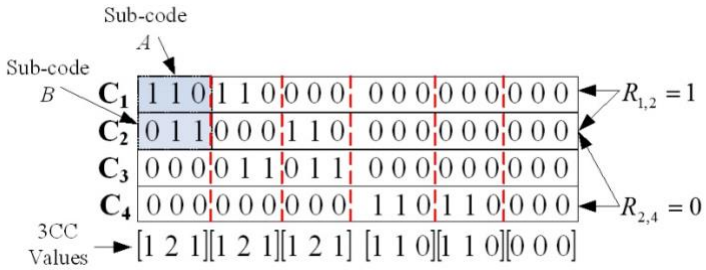

FIG. 13: KS codes illustrating 3CC and values.

When the number of requesting nodes having the same weight (sensors in the same region) is equal to the maximum number of users for that particular mapping, $K_W = K_{max}(M)$, a fixed mapping technique is the best choice for VW-KS codes. In the case of $K_W < K_{max}(M)$, a dynamic weight assignment technique can be result in a reduced code length and utilised bandwidth, provided that the number of mappings is one, i.e. $M = 1$. However, for $M > 1$, a combination of both techniques results in better bandwidth utilisation. In this method, it is important to determine the number of maximum nodes in the previous mapping, $K_{max}(M-1)$. For large number of requesting users, K_W, where the number of mapping is greater than one ($M > 1$), fixed mapping technique is the best choice for nodes up to $K_{max}(M-1)$. While for the remaining users, $K_r = K_W - K_{max}(M-1)$, their codes can be constructed using dynamic weight assignment. The codes of different weights, generated using fixed mapping for $1 \leq K_W \leq K_{max}(M-1)$ are appended diagonally, and later combined with codes for remaining users, K_r generated using dynamic weight assignment technique. The general form of the hybrid fixed-dynamic weight assignment technique is depicted in Figure 14 and its code length is given by

$$N_V = \left\lceil \sum_{q=1}^{Q} \sum_{k=1}^{K_{max}(M-1)} N_{r,q} + \frac{3}{4} \sum_{q=1}^{Q} K_{r,q} W_q \right\rceil \tag{A.2}$$

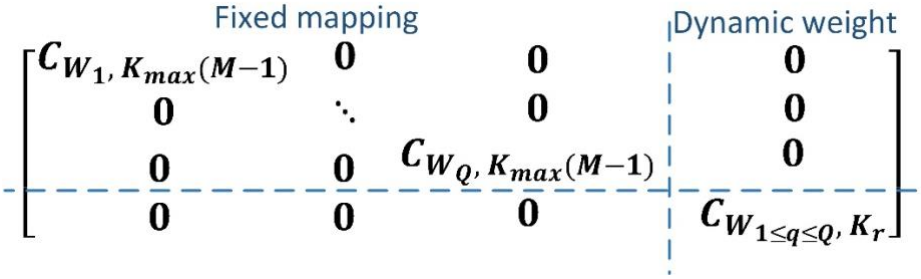

FIG. 14: General form of hybrid fixed-dynamic weight assignment technique.